Astron. Astrophys. 322, 523–532 (1997)

ASTRONOMY
AND
ASTROPHYSICS

Cascade initiated by VHE γ-rays in the radiation field of a close massive companion

W. Bednarek

Department of Experimental Physics, University of Lódź, ul. Pomorska 149/153, PL-90236 Lódź, Poland

Received 13 September 1996 / Accepted 4 December 1996

Abstract. Two massive binaries, Cyg X-3 and LSI 303^o+61, are inside the error boxes of γ-ray sources detected by the Compton GRO. If somewhere inside such binary systems are injected very high energy (VHE) γ-rays, as suggested by some Cherenkov observations, they may initiate the inverse Compton $e^{\pm}$ pair cascade in the soft radiation of a massive companion, and the detected high energy γ-ray emission may be caused by the secondary γ-rays of such cascade process. Since VHE γ-rays has to propagate in the anisotropic radiation of a massive star (the place of injection does not cover with the source of soft radiation), the intensities of secondary γ-rays depend on the angles of observation measured from direction defined by the place of injection of VHE γ-rays and the center of a massive star. We compute γ-ray spectra formed in such anisotropic cascade by using the Monte Carlo method. It is found that the intensity of secondary γ-rays does not varies strongly for the angles of observation greater than $\sim 90^o$, but the highest intensities are observed at the angles corresponding to the limb of a massive star. Moreover, some cascade γ-rays can also emerge from behind the massive star, i.e. from the opposite site than the location of a source of primary γ-rays. This interesting feature can be called as a *focusing of γ-rays by the soft radiation of a massive star.*

Key words: gamma-rays: general – stars: binaries: close – stars: individual: LSI+61^o303, Cyg X-3

1. Introduction

The observations of VHE γ-rays from directions of some X-ray binaries has been claimed frequently during last two decades (see for the review e.g. Weekes, 1989, 1992). Although that results are at present in some doubt, the production of γ-rays in the systems which contain a compact object (neutron star or black hole) and a massive companion is frequently discussed in the literature. For example, γ-rays can be produced by particles accelerated by young pulsars which are members of binary systems, or by particles accelerated by a shock which is formed in collisions of stellar and pulsar winds inside the massive binaries containing a compact object (e.g. Bignami, Maraschi & Treves 1977, Bednarek et al. 1990, Harding & Gaisser 1990) or massive binaries of early-type stars (e.g. in WR 140; Eichler & Usov 1993).

Recent observations of X-ray binaries by detectors on the Compton GRO, below $\sim$ 30GeV, shows that two γ-ray sources are coincident with the high probability with massive binary systems. First one, is the massive binary system LSI+61^o303, which is also a variable strong radio source (GT 0236+610). It has been observed by the COMPTEL detector, three times during the first year of observations (Phase I), showing the flat spectrum with index ~ 1.7 in the energy range 1-30 MeV (van Dijk et al. 1993), and the flux which do not change significantly between observations. At higher energies the EGRET detector confirmed the existence of the COS B source 2CG 135+01 (Hermsen et al. 1977) coincident with LSI+61^o303 with the spectral index $\sim 1.9 \pm 0.1$ above 100 MeV (2EG J0241+6119, Thompson et al. 1995). The second source is the famous Cyg X-3, which has been claimed as a γ-ray source by the SAS-2 satellite (Lamb et al. 1977; Fichtel et al. 1987), whereas not observed by the COS B experiment (Hermsen et al. 1987). Recent observations by the EGRET detector show, that the γ-ray source, 2EG J2033-4112, is positionally coincident with Cyg X-3 (Merck et al. 1995). However the γ-ray emission is not modulated with the orbital period of the binary system, in contradiction to the strong modulation observed in X-rays. This fact is interpreted, that no confirmation of γ-ray emission by the Cyg X-3 can be claimed. Surprisingly, the Second EGRET Catalog (Thompson et al. 1995) reports that the spectral index of 2EG J2033-4112 is $\sim 1.9 \pm 0.1$, which differs significantly from the Galactic diffuse γ-ray spectrum but is this same as in the case of 2EG J0241+6119, coincident with LSI+61^o303.

We wonder if the strong modulation of high energy γ-ray emission with the massive binary orbital period has to be really expected. In this paper, we consider the standard model in which the VHE γ-ray photons are produced somewhere in the binary system but, relatively close to a massive companion. These γ-rays can be absorbed by the soft radiation of a massive star. The

Send offprint requests to: Bednar@krysia.uni.lodz.pl

secondary $e^{\pm}$ pairs, produced in this process, may comptonize the star radiation into the γ-ray energy range. However, the angular distribution of the ICS γ-rays can be much more isotropic than that one of primary VHE γ-rays if the secondary $e^{\pm}$ pairs are isotropised by the magnetic field of the massive star. The necessary condition for such a picture to occur is the absorption of primary VHE γ-rays in the massive star radiation. The optical depth for the VHE γ-rays in such general scenario has been recently computed by Moskalenko, Karakula & Tkaczyk (1993), neglecting the radius of the massive star in respect to the distance at which the primary γ-rays are injected. However, with such assumption the computations are valid only for photons propagating far away from a massive star where the density of star soft photons is low and the absorption effects are small. So then, their approximation is rather pure for close binaries and may introduce some artifacts in the form of very narrow absorption features in the light curves of these sources. Moreover, the $e^{\pm}$ inverse Compton cascade which can be initiated by the secondary $e^{\pm}$ pairs, originated in the γ-ray - soft photon collision, is not considered in that paper. Here we want to address this last problem in details. In Sect. 2 we compute the optical depth for the γ-ray photons in the star radiation taking into consideration the star dimensions and discuss the general conditions for the development of such cascade. The details of Monte Carlo simulations of the cascade are shown in Sect. 3. We compute the angle dependent γ-ray spectra escaping from the binary system and discuss them in Sect. 4. The paper finish with conclusions and short discussion of the applicability of such a model to two binary systems LSI+61^{o}303, and Cyg X-3 (Sect. 5).

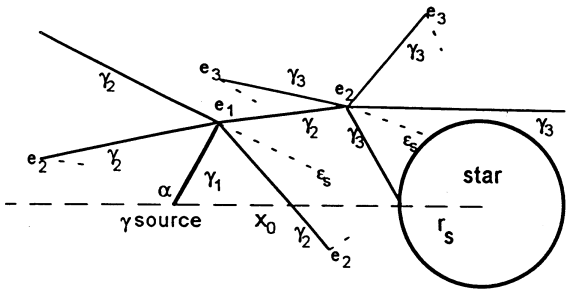

Fig. 1. Schematic view of the development of a cascade initiated by γ-ray photon in the soft radiation field of a massive star. The γ-ray (γ_1) escapes from a 'γ source', which is at a distance x_0 from the center of a massive star, at an angle α. It produces an $e^{\pm}$ pair (e_1) in collision with the massive star thermal photon (ϵ_s). The $e^{\pm}$ pair emits secondary γ-rays (γ_2) in the inverse Compton scattering process of soft star photons. These secondary γ-rays may: (a) escape form the system, (b) collide with the massive star surface, or (c) create next $e^{\pm}$ pair (e_2). The process continues up to the moment when all secondary γ-rays escape from the system or collide with the star surface, and all secondary $e^{\pm}$ pairs cool.

2. Propagation of VHE γ-ray in the radiation field of a massive star

Let us assume that VHE γ-ray photon with energy E_γ is injected a distance x_0 from the center of a massive star and propagates at an angle α, measured from the direction to the star (see Fig. 1). The star has a radius r_s and emits black body radiation with temperature T_s. The picture is axially symmetric with the main axis covering with the direction x_0. If the star is very luminous and the γ-ray is injected relatively close to its surface, it may create an $e^{\pm}$ pair in collision with soft star photons. The secondary $e^{\pm}$ pairs lose energy on different processes but, in the case when the inverse Compton scattering (ICS) of star photons dominates, the cascade in an anisotropic radiation field can develop (Fig 1). In the following subsections we discuss the conditions for such a cascade to occur.

2.1. Optical depth for the γ-ray photon in the radiation field of a massive star

The optical depth for the γ-ray photon propagating in the soft photon field can be computed following the formula given by Gould & Schreder (1967). The way how to compute it in our specific case of the anisotropic soft photon field coming from the star surface is shown in Appendix A. Here we present some results of the numerical computations of the optical depth for the parameters of a massive star which seems to be characteristic for close massive binaries (see e.g. Moffat & Marchenko 1996). Fig. 2a shows the dependence of the optical depth for the γ-ray photon with energy 10^{12}eV on the angle of photon injection α for selected distances x_0 from the star. As expected, the optical depth is higher for larger values of the angle α up to the moment of collision of the photon path with the star surface. If the injection angle α passes the angle at which the star limb is seen (α_s), the optical depth drops drastically. For $\alpha > \alpha_s$, the optical depth decreases slightly because the propagation distance of the γ-ray photon to the moment of collision with the star surface becomes shorter but the geometrical effects do not play important role in such a case. The optical depth decreases with the distance of injection of γ-ray photon from the star surface x_0 for small angles α but the maximal value of the optical depth, corresponding to the marginal collision with the star surface, increases with x_0 because of the propagation distance in the star radiation is higher. In Fig. 2b the dependence of the optical depth on the energy of γ-ray photon is shown for selected angles of photon injection α. As expected from the kinematics of the ICS process, the maximum in the optical depth shifts to lower γ-ray photon energies and its absolute value increases with increasing angle α, if $\alpha \in (0^o; \alpha_s)$, where $\alpha_s \approx 151^o$ for the parameters in Fig. 2b. For the angles $\alpha > \alpha_s$, the location of the maximum in the optical depth do not change with energy of the γ-ray photon since the γ-ray propagates towards the surface of the star. However the value of the optical depth drops for higher α since the propagation distance of γ-ray photon from the place of its injection up to the collision with the star surface is shorter.

Based on the computations of the optical depth we are able to determine the observable parameters of massive stars (its luminosity L_s and surface temperature) for which the absorption of the γ-rays can become important. The optimal absorption

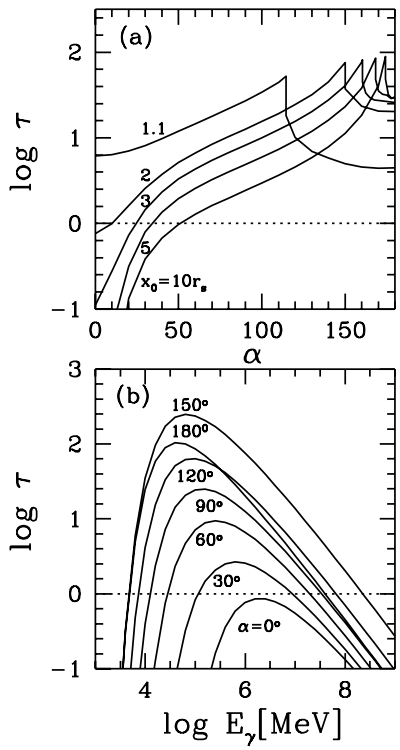

Fig. 2. a The optical depth for the γ-ray photon with energy $E_\gamma = 10^{12}$ eV in the soft radiation of a massive star, as a function of the angle of photon injection α. The star has the radius $r_s = 2 \times 10^{11}$cm and the surface temperature $T_s = 9 \times 10^4$K. The specific curves correspond to different distances of injection of the primary photon from the center of a star $x_0 = 1.1, 2, 3, 5$, and $10r_s$. **b** The optical depth for the γ-ray photons, as a function of their energy E_γ, which are injected at the distance $x_0 = 2r_s$. Specific curves correspond to different angles of photon injection α.

conditions occur for the γ-ray photons, with energy E_γ^{opt}, which propagate along the path tangent to the star limb. This photon energy E_γ^{opt} is approximately given by the threshold condition for the absorption of γ-ray, $E_\gamma^{opt} \approx 4m_e/3kT_s$, where m_e is the electron mass and k is the Boltzman constant. The optical depth for the γ-ray photon is proportional to $\propto T_s^3 r_s$ and the star luminosity to $\propto T_s^4 r_s^2$. Therefore, the star parameters has to fulfil the following condition,

$$L_s^{\tau=1} T_s^2 \approx A, \tag{1}$$

provided that the optical depth is equal to one for the limb crossing γ-ray. In this relation L_s is expressed in erg s^{-1}, T_s in Kelvins, and A is a constant weakly dependent on the distance x_0 above $x_0 \sim 2r_s$. The value of A has been computed numerically and is plotted in Fig. 3 as a function of x_0/r_s. The γ-ray photons with energies above the threshold for $e^\pm$ pair production in collision with soft photons can be absorbed in the radiation field of the massive star if its luminosity $L_s \gg L_s^{\tau=1}$.

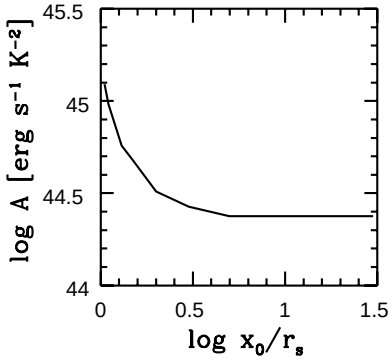

Fig. 3. The dependence of A on the distance x_o from the center of a star.

2.2. General conditions for the development of an ICS cascade

The ICS cascade can be initiated by a VHE γ-ray in the vicinity of a specific massive star if the ICS losses of secondary $e^\pm$ pairs dominates the electron losses on synchrotron and bremsstrahlung processes. The ratio of ICS $e^\pm$ pair losses in the Thomson limit to synchrotron losses is determined by the energy densities of the star radiation U_{rad} and the magnetic field U_B. At the star surface is given by

$$U_{rad}/U_B \cong 10^{-11} D_s T_s^4 B_s^{-2}, \tag{2}$$

where B_s is the magnetic field at the star surface (in Gauss), and $D = \Delta\Omega/4\pi$ is the dilution factor of the star radiation which for isotropic electrons can be defined as a part of the sphere which is obscured by the star. For the star surface $D_s = 0.5$. The ICS losses dominates if the star surface magnetic field is

$$B_s < B_T \approx 3 \times 10^{-6} D_s^{0.5} T_s^2. \tag{3}$$

However, this limit is valid only in the Thomson regime. In general case, we have to compute the ICS losses of electrons in the radiation of a massive star using the full Klein-Nishina cross section. The comparison of these losses with the electron losses on synchrotron process gives the limit on the star magnetic field (B_s) which is more restrict for the electrons with very high energies. This critical value of B_s is shown in Fig. 4 as a function of electron's energy, after its normalization to B_T.

The upper limits on the surface magnetic field of massive stars are of the order of a few hundred Gauss, for OB stars (Barker 1986), up to $\sim 10^4$ G, for the Wolf-Rayet stars (Maheswaran & Cassinelli 1988). The magnetic field of the stars drops with distance as r^{-2}, for the stars with strong winds, or even faster, e.g. if the star magnetic field can be considered as a dipole (Weber & Davis 1967; Usov & Melrose 1992). So then, if the radiation energy density dominates on the star surface, it has to dominate above the star surface as well. For example, for the parameters of the massive star in Cyg X-3 system (Moffat & Marchenko 1996): $r_s \cong 10^{11}$cm, $T_s \cong 9 \times 10^4$K, the ICS losses in the Thomson limit dominates over synchrotron losses if $B_s \leq 2 \times 10^4$ G. This value is above the observational limits on the surface magnetic fields of Wolf-Rayet stars.

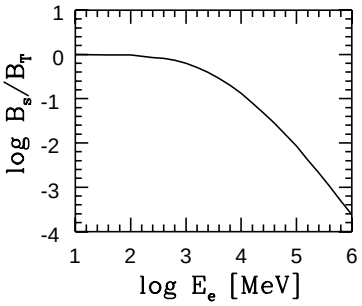

Fig. 4. The dependence of the surface magnetic field of a massive star, below which the ICS losses of electrons dominates over the synchrotron losses, on the electron energy $E_{e^\pm}$. The magnetic filed is normalized to the value of the magnetic field for which the ICS losses of electrons in the Thomson regime are equal to their synchrotron losses.

It is necessary to check also if for typical parameters of massive companions, the electron energy losses on bremsstrahlung process do not dominate the ICS losses. Since the wind density and the radiation density drops with the distance from the star in this same way ($\propto r^{-2}$), it is enough to compare these losses at the star surface. It can be simply derived that the ICS losses in the Thomson limit dominate for electrons with the Lorentz factors

$$\gamma \geq \gamma_{brem} = 2 \times 10^{54} m_{loss} v_{wind}^{-1} r_s^{-2} T_s^{-4} D^{-1}, \quad (4)$$

where r_s, T_s, v_{wind}, and m_{loss} are the radius (in cm) and the surface temperature of the massive star, its wind velocity (in cm s^{-1}), and the mass loss rate of the star (in $M_\odot yr^{-1}$), respectively. Applying the typical parameters of the Wolf-Rayet stars, used above, and assuming the wind velocities of the order of $v_{wind} \cong$ 3000km s^{-1}, and $m_{loss} \cong 10^{-5} M_\odot yr^{-1}$, we obtain that Eq. (4) is fulfilled for electrons with arbitrary Lorentz factors. So then, the bremsstrahlung losses of electrons are negligible in comparison to ICS losses.

In our picture we assume that the secondary cascade electrons are isotropised locally, i.e. in the place of their birth. It is true if the distance scales λ_{ICS} for the ICS energy losses of secondary electrons are longer than their Larmor orbits R_L in the local magnetic field, $2\pi R_L < \lambda_{ICS}$. This condition is fulfilled if the local random magnetic field,

$$B_r \geq 4 \times 10^{-29} \gamma^2 T_s^4 D. \quad (5)$$

For example, for $T_s = 10^5$K, $\gamma = 10^4$ (corresponds to the minimal value of λ_{ICS}, which is on the border between the Klein-Nishina and the Thomson regimes), and for $D_s = 0.5$, the magnetic filed has to be $B_r \geq$ 1.6Gs. If the scattering of the star photons by secondary electrons occurs in the Klein-Nishina regime, the electron attenuation length and the Larmor radius increases in a similar way with the electron Lorentz factor γ, and $R_L/\lambda_{ICS} \approx const$. This means that if the condition for isotropisation of electrons is fulfilled in the Thomson limit (Eq. 5), it has to be valid in the Klein-Nishina regime as well.

To summarise, our picture for the ICS cascade, developing in the radiation field of a massive star, is valid for the massive stars with the surface magnetic field limited by Eq. (3) and (5), and if the secondary $e^\pm$ pairs have the Lorentz factors above γ_{brem} (Eq. 4).

3. Description of Monte Carlo simulations of the cascade process

In order to find out if the γ-ray photon can produce an $e^\pm$ pair in collision with a soft star photon we have to know the propagation distance for this γ-ray in the anisotropic radiation of the star. The details of computations of the reciprocal of the propagation distance $\lambda_{\gamma\gamma}(E_\gamma, x_0, \alpha_0)$ in our picture are given in Appendix A. The distance l_γ at which the γ-ray converts into the $e^\pm$ pair can be found by choosing the random number P_1 and sampling from

$$P_1 = \int_0^{l_\gamma} \lambda_{\gamma\gamma}^{-1}(E_\gamma, x_\gamma, \alpha_\gamma) e^{-l/\lambda_{\gamma\gamma}(E_\gamma, x_\gamma, \alpha_\gamma)} dl \quad (6)$$

If this condition can not be fulfilled for chosen random number P_1, we accept that the γ-ray escapes from the star radiation field or collides with the star surface. Simple trigonometry allows us to determine the distance of produced $e^\pm$ pair, $x_{e^\pm}$, from the center of a massive star. The energy of created electron (positron) is chosen by sampling from the differential spectrum of pairs which can be produced by the γ-ray photon at a propagation distance l_γ. The details of computation of this spectrum are given in Appendix B. Choosing the random number P_2, the energy of electron E_e is obtained from

$$P_2 = \left(\int_{0.5}^{E_e} \frac{dW}{dEdx} dE \right) \left(\int_{0.5}^{E_{e,max}} \frac{dW}{dEdx} dE \right)^{-1} \quad (7)$$

where $dW/dEdx$ is defined by Eq. (B1) in Appendix B, and $E_{e,max}$ is the maximal possible energy of the electron produced in γ-ray soft photon collision. The energy of positron is then $E_p = E_\gamma - E_e$.

We assume further that the $e^\pm$ pairs created by the γ-ray photon are locally isotropised by the random component of the magnetic field. The conditions for that to occur are discussed in Sect. 2. The pairs cool locally and produce the next generation of γ-rays in the inverse Compton scattering of soft photons coming from the massive star. The problem appears how to chose directions and energies of secondary ICS γ-rays. In order to select the direction of the secondary γ-ray we compute at first the energy loss rate on ICS for pairs with energy $E_{e^\pm}$ assuming that the electron (positron) is located at the distance $x_{e^\pm}$ and propagates at an angle $\alpha_{e^\pm}$ to the direction defined by $x_{e^\pm}$. The details of the computations of electron energy losses in such case are given in Appendix C. The direction of motion of a secondary γ-ray, which is in fact for relativistic electrons this same as the direction of the electron in the moment of production of γ-ray photon in ICS process, is obtained by sampling from the distribution of the energy loss rates computed as a function of the angle $\alpha_{e^\pm}$ after its normalization to the total energy loss rate for electrons moving isotropically at $x_{e^\pm}$. Choosing the

random number P_3 we can define the cosine of the angle of γ-ray emission ($\cos\alpha_\gamma$) from

$$P_3 = \left(\int_{\cos\alpha_\gamma}^{1} \frac{dL}{dtd\nu}d\nu\right)\left(\int_{-1}^{1} \frac{dL}{dtd\nu}d\nu\right)^{-1}, \quad (8)$$

where

$$\frac{dL}{dtd\nu} = \int_0^{E_{\gamma,max}} \frac{dN}{dtdE_\gamma}\frac{dN_{e^\pm}}{d\nu}E_\gamma dE_\gamma, \quad (9)$$

$dN/dtdE_\gamma$ is the photon spectrum produced by electrons in ICS process (for details of computations see Appendix C), $dN_{e^\pm}/d\nu$ describes the number of electrons moving in unit cosine angle $d\nu = d(\cos\alpha)$, and $E_{\gamma,max}$ is the maximum energy of the γ-ray photon produced in the ICS process by an electron with energy $E_{e^\pm}$, located at the distance $x_{e^\pm}$, and propagating at the angle $\alpha_{e^\pm} = \alpha_\gamma$.

Since the process is symmetrical in respect to the direction defined by $x_{e^\pm}$, we can select the azimuthal angle ϕ needed to define the photon direction in spherical coordinates, after choosing the random number P_4,

$$\phi_\gamma = 2\pi P_4. \quad (10)$$

Having selected randomly the direction of motion of the ICS γ-rays, we have to determine their energies. To save the computing time we accept that the energy of γ-ray photon E'_γ produced by an electron with energy $E_{e^\pm}$, which propagates at a distance $x_{e^\pm}$ and at an angle α_γ, is equal to the mean value defined by the relation

$$< E_\gamma > = \left(\frac{dL}{dtd\nu}\right)\left(\frac{dN}{dtd\nu}\right)^{-1}, \quad (11)$$

where

$$\frac{dN}{dtd\nu} = \int_0^{E_{\gamma,max}} \frac{dN}{dtdE_\gamma}\frac{dN_{e^\pm}}{d\nu}dE_\gamma \quad (12)$$

is the rate of photon production by an electron in the ICS process. As an example, we show the dependence of $< E_\gamma >$ on $E_{e^\pm}$ for different angles of electron propagation α and two distances from the center of the star $x_0 = 2r_s$ (Fig. 4a) and $10r_s$ (Fig. 4b). Note that the average energy of ICS γ-rays does not change significantly with the distance from the massive star for the angles α significantly higher than the angular size of a massive star $\alpha > \pi - \alpha_s$. However, the geometrical effects on ICS process are important for $\alpha \leq \pi - \alpha_s$.

The above described procedure is repeated for all cascade pairs up to the moment of their 'complete cooling', i.e. that they are not able to produce the γ-ray photons in ICS process with energies above certain applied value. In our simulations these critical energy for secondary γ-ray photons has been chosen as equal to 10 MeV. The parameters of the ICS γ-rays, which are above the threshold for $\gamma\gamma \rightarrow e^\pm$ pair production, are stored and then the cascade procedure is repeated for each of them as it has been described above for the primary γ-ray. The ICS γ-rays which are below this threshold, are added to the store of escaping cascade γ-rays or γ-rays colliding with the massive star, after their sorting in angle and energy bins.

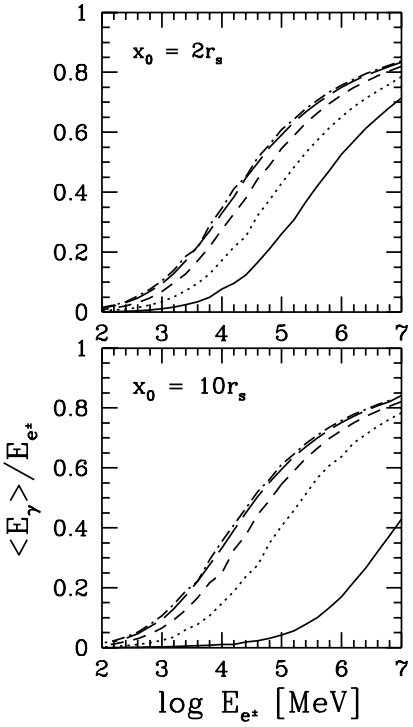

Fig. 5a and b. The dependence of the average photon energy $< E_\gamma >$, produced by an electron in the ICS process, on the electron energy $E_{e^\pm}$. Electrons are injected at the distance $x_0 = 2r_s$ **a** and $10r_s$ **b** from the center of a massive star with the radius $r_s = 2 \times 10^{11}$ cm and surface temperature $T_s = 9 \times 10^4$K. Specific lines correspond to different angles α of the electron propagation in respect to the direction defined by x_0: $\alpha = 0^o$ (full line), 45^o (dotted line), 90^o (dashed line), 135^o (long-dashed line), and 180^o (dot-dashed line).

4. Results of Monte Carlo simulations

We follow the cascade initiated by monoenergetic primary γ-rays. The secondary cascade γ-ray spectra depend on the angle of their escape from the vicinity of a massive star (θ), which is measured from the direction defined by the place of injection of primary γ-rays and the center of a massive star (see Fig. 1). All sphere is divided on 10 parts with the width of 0.2 measured in $\cos\theta$. It is assumed that the secondary γ-rays are removed from the cascade if they move outside $30r_s$ or collide with the massive star surface. The secondary γ-rays with energies above 10MeV are sorted into bins with the width of 0.2 in log scale. Limited computing facility pressed us to present the average results which base only on 10 simulations for the primary γ-rays with energy $E_\gamma = 10^6$MeV (accept for $\alpha = 0^o$, which base on 20 simulations), and on 50 simulations for $E_\gamma = 10^5$MeV (accept for $\alpha = 0^o$, which base on 10^4 simulations). However, even for such small number of simulations the results show reasonable stability within several percent. All simulations discussed in this section has been obtained for a massive star with the surface temperature $T_s = 9 \times 10^4$K and the radius $r_s = 2 \times 10^{11}$cm. Such a massive star is probably present in the Cyg X-3 binary system (van Kerkwijk et al. 1992; Moffat & Marchenko 1996).

In order to investigate the dependence of secondary cascade γ-ray spectra on the observation angle θ, the simulations for injection angle $\alpha = 0^o$ and 180^o have been performed for the primary γ-rays with energies $E_\gamma = 10^6$ and 10^5MeV, but for fixed distance from a massive star $x_0 = 2r_s$. In Fig. 6 we show the secondary γ-ray spectra which escape within the intervals $\cos\theta = 0.8 \div 1; 0.4 \div 0.6; -0.2 \div 0; -0.8 \div -0.6; -0.8 \div -1$. The intensities of γ-rays, escaping in unit solid angle, change significantly with the observation angle θ (by about one and a half decade). The lowest intensities correspond to the smallest values of angle θ (full line in Fig. 6) but the highest to the angles of θ close to the angle defined by the star limb α_s, which for the injection distance $x_o = 2r_s$ is equal to $\cos\alpha_s \cong -0.866$. This feature becomes clear if we remind ourself that the production of γ-rays in ICS scattering preferentially occurs when the secondary electron propagates towards the source of soft photons, i.e. to the surface of a massive star. From this same reason, the essential number of cascade γ-rays is able to emerge even from the opposite site of the massive star than the position of a source of the primary γ-rays. This case corresponds to the interval $\cos\theta = -0.8 \div -1$ (see dot-dashed curves in Fig. 6). So then, the soft radiation of a massive star can play a role of focusing lens for the source of primary γ-rays. The intensities of γ-rays, escaping within the range of angles $\cos\alpha \approx 0. \div -0.8$, are comparable within a factor of 2 (see long- and short dashed, and dot-dashed curves in Fig. 6). Therefore, we expect that the external observer should not detect strong modulation of the γ-ray signal in essential part of the orbital period of the binary system, provided that the source of primary γ-rays is on close to circular orbit. The shapes of secondary γ-ray spectra, emerging at different angles, are very similar to each other. They have differential photon spectral index close to ~ 1.5 with a cut-off at approximately $\sim 10^4$MeV, which is determined by the massive star surface temperature (in these computations $T_s = 9 \times 10^5$K). However, more detailed analysis of results shows that the γ-ray spectra cuts-off at slightly higher energies for smaller angles θ, which is clear, since the secondary γ-rays, escaping at smaller angles, are produced on average after smaller number of cascade generations.

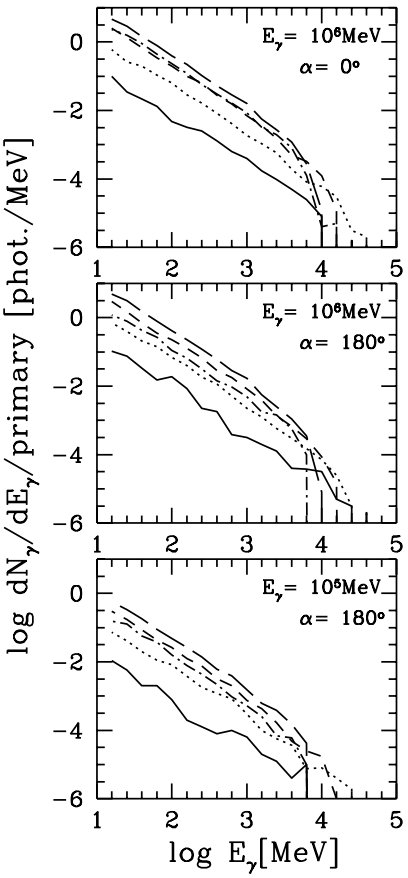

Fig. 6. The average spectra of secondary cascade γ-rays which escapes from the vicinity of a massive star at different angles θ. Specific curves show the spectra of γ-rays escaping at the angles $\cos\theta = 0.8 \div 1.$ (full line), $\cos\theta = 0.4 \div 0.6$ (dotted line), $\cos\theta = -0.2 \div 0.$ (dashed line), $\cos\theta = -0.6 \div -0.8$ (long-dashed line), and $\cos\theta = -1. \div -0.8$ (dot-dashed line). The cascade is initiated by the monoenergetic γ-ray photons with energies E_γ, injected at the distance $x_0 = 2r_s$ and the angle α.

We investigate also the dependence of escaping γ-ray spectra on the angle of injection α of primary γ-rays. The results of such computations are presented in Fig. 7 for the γ-rays escaping inside the cosine intervals $\cos\theta = 0.8 \div 1, 0 \div 0.2$, and $-1 \div -0.8$, assuming that the cascade is initiated by the primary γ-rays with energies $E_\gamma = 10^6$MeV (on the left) and 10^5MeV (on the right), at the angles $\alpha = 0^o, 45^o, 90^o, 135^o$, and 180^o degrees. For the primary γ-rays with energies $E_\gamma = 10^6$MeV, the spectra and their intensities are remarkable similar to each other. This feature reflects the fact that if only the optical depth for the primary γ-ray is of the order of unity (or higher), the interaction with the star photon occurs close to the place of their injection, and the conditions for further cascade development are similar. This is exactly the case for $E_\gamma = 10^6$MeV and $x_o = 2r_s$ (see Fig. 2a). From this same reason, the γ-ray with energy $E_\gamma = 10^6$MeV, but injected at $x_o = 10r_s$, produces similar distributions of secondary γ-ray spectra only for injection angles $\alpha \geq 50^o$ (Fig. 2a).

Another interesting similarity occurs between the angular distributions of secondary spectra produced by γ-rays with different energies, e.g. 10^6MeV and 10^5MeV (in Fig. 7, results presented on the left and on the right side, respectively). Careful look on Fig. 2b allows to understand this feature. The angular distributions of γ-rays are determined by the cascade γ-rays which reaches unity for a given angle α. For primary γ-rays with energies 10^5MeV, it occurs for the angles $\alpha \geq 30^o$ (Fig. 2b). This means that, when comparing the distributions caused by the primary γ-rays with energies 10^6 and 10^5MeV, they should be similar if the angles of injections are above $\alpha \approx 30^o$, but should differ from each other for smaller angles.

Because of the focusing effect of the γ-rays mentioned above, a significant part of secondary γ-rays, more than expected from simple geometrical considerations, collide with the surface of a massive star. The spectra of colliding γ-rays, and

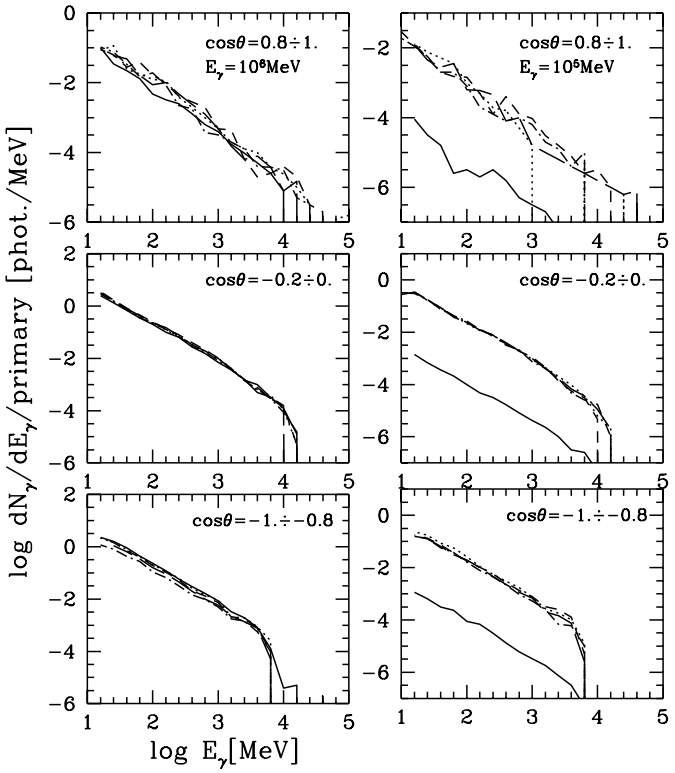

Fig. 7. The spectra of secondary cascade γ-rays which escape at fixed intervals of the angle θ equal to: $\cos\theta = 0.8 \div 1, 0. \div 0.2$, and $-1 \div -0.8$, but for different angles of injection of monoenergetic γ-rays: $\alpha = 0^o$ (full line), 45^o (dotted line), 90^o (dashed line), 135^o (long-dashed line), and 180^o (dot-dashed line). The figures on the left are for the primary γ-rays with energy $E_\gamma = 10^6$MeV and that ones on the right are for $E_\gamma = 10^5$MeV.

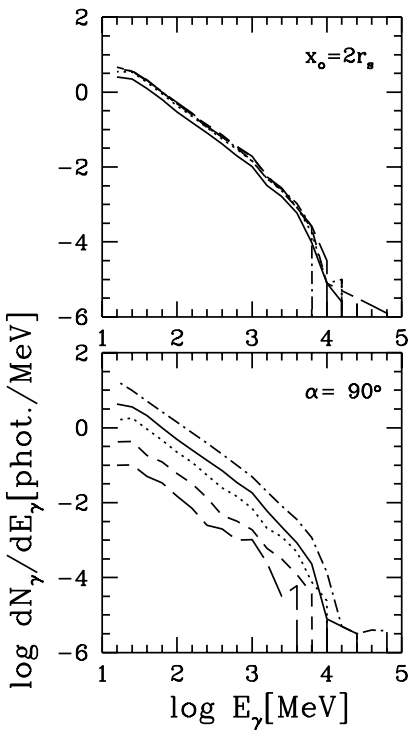

Fig. 8a and b. The spectra of secondary cascade γ-rays, initiated by the monoenergetic γ-rays with energy $E_\gamma = 10^6$MeV, which collide with the surface of a massive star. Specific curves in **a** show the spectra for the primary γ-rays injected at $x_0 = 2r_s$ but for different $\alpha = 0^o$ (full line), 45^o (dotted line), 90^o (dashed line),135^o (long-dashed line), and 180^o (dot-dashed line). In **b**, such γ-ray spectra are shown for $x_0 = 1.1$ (dot-dashed line), 2 (full line), 3 (dotted line), 5 (dashed line), and $10r_s$ (long-dashed line) and the angle $\alpha = 90^o$.

their power transferred to the massive star, very strongly depend on the distance of injection of primary γ-ray photons (Fig. 8b, and Table. 1, where the power of γ-rays colliding with the star is computed for the fixed distance of injection of primary γ-rays $x_o = 2r_s$ and different angles α, and for the fixed angle $\alpha = 90^o$ and different distances). However, the dependence of colliding γ-ray spectra and their power on the angle of injection of primary γ-rays is small (Fig. 8a). It is interesting that for the primary γ-rays injected tangentially ($\alpha \approx 90^o$) and very close to the surface of a massive star, as postulated by some models of VHE γ-ray production in X-ray binary systems(e.g. Vestrand & Eichler 1982), almost half of the power of secondary γ-rays is transferred to the surface of a massive star (see Table. 1, results for $x_o = 1.1r_s$).

In Fig. 9, the dependence of escaping phase averaged secondary γ-ray spectra, i.e. integrated over the angles of observations, on the parameters of the injected primary γ-rays is shown. It is found that, even if the distance of the γ-ray source from a massive star changes significantly during the orbital period, the intensities of the phase averaged secondary γ-ray spectra change only by a factor of two and the total power of escaping γ-rays by only several percent (see Fig. 9, and Table. 2). However, the cut-offs in these spectra essentially increase with the distance from a massive star.

Table 1. Fraction of energy of primary γ-rays in % which is absorbed by the massive star

$E_\gamma[MeV]$	$\alpha = 0^o$	45^o	90^o	135^o	180^o
10^6	7.6	11.3	13.4	15.5	25.6
10^5	0.05	12.2	11.5	13.8	18.5
E_γ	$x_o[r_s] = 1.1$	2.	3.	5.	10.
10^6	45.3	13.4	5.8	1.4	0.52
10^5	44.2	11.5	5.4	1.8	0.49

The general tendency can be noticed that if the primary γ-rays are injected relatively close to the star ($x_o \leq 2r_s$), the spectra of secondary cascade γ-rays colliding with the star cuts-off at higher energies than the phase averaged γ-ray spectra escaping from the system (compare the results in Figs. 8 and 9). Opposite tendency is observed for the γ-rays injected further from the massive star ($x_o > 2r_s$). This feature is explained by the fact that, on average, the lower energy secondary γ-rays are produced after higher number of cascade generations. Colliding γ-rays are produced after higher number of generations then

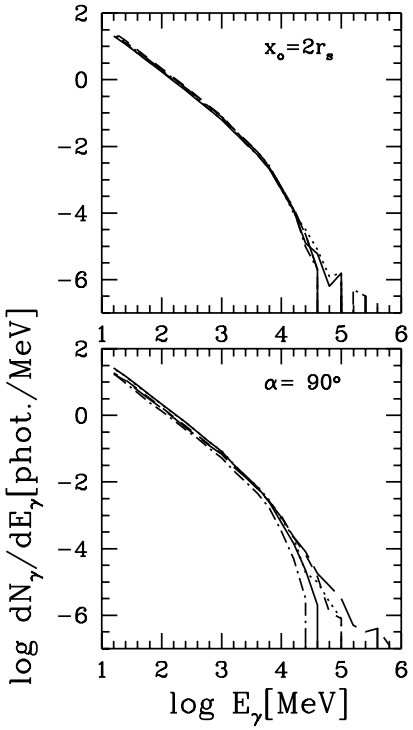

Fig. 9a and b. The spectra of secondary γ-rays produced in the cascade, averaged over θ (phase averaged). The computations have been performed for these same parameters as in Fig. 8.

Table 2. Fraction of energy of primary γ-rays in % which escapes from the binary system

$E_\gamma[MeV]$	$\alpha = 0^o$	45^o	90^o	135^o	180^o
10^6	89.94	84.3	83.7	81.9	71.9
10^5	99.935	85.4	82.7	78.5	79.1
E_γ	$x_o[r_s] = 1.1$	2.	3.	5.	10.
10^6	51.4	83.7	92.0	98.5	98.8
10^5	52.0	82.7	92.5	94.0	97.7

escaping γ-rays if the primary VHE γ-rays are injected further from a massive star.

5. Conclusion

If the VHE γ-rays are injected somewhere inside massive binary systems, they may initiate the inverse Compton pair cascade in the anisotropic radiation of a massive companion, provided that the ICS losses of secondary cascade $e^{\pm}$pairs dominates over other energy losses. The conditions for that to occur are determined in Sect. 2. The spectra of escaping secondary cascade γ-rays depend on the angle of observation θ, but in quite broad range of the angles this dependence is not strong which may create problems with detection of the modulation of the γ-ray signal with the orbital periods of such massive binaries. There are some other interesting predictions of our model which might be tested by the future sensitive observations of massive binaries. For example, we expect that the highest level of γ-ray emission, detected in the Compton GRO energy range, should be observed when the source of primary VHE γ-rays is passing the limb of a massive star. The low level emission should be also observed even if the source is located behind a massive star (effects of *focusing of the γ-ray emission by the soft radiation of a massive star*).

In fact the ICS cascade, discussed above, does not need to occur in all volume of the massive binary systems. In some regions the magnetic field may be enhanced, e.g. as a result of compression caused by the shock waves, or it may be connected with the Solar type active regions on the surface of a massive star. In such regions the secondary cascade $e^{\pm}$ pairs lose energy mainly on synchrotron process emitting low energy photons.

The secondary positrons, created in the discussed cascade, and the positrons produced by the γ-rays colliding with a massive star (Table 1), should annihilate after slowing down. Depending on the conditions in the binary system and on the surface of a massive star, they may form a broad or narrow annihilation feature. Therefore our model predicts the appearance of a weak annihilation feature connected with the γ-ray emission from massive binaries. Note that observation of a narrow annihilation line has been reported from the massive binary Cyg X-1 (Ling & Wheaton 1989). This interesting problem will be discussed in detail in the next paper (Bednarek et al. 1996).

Two binary systems, probable γ-ray sources, fulfils the condition (Eq. 1) necessary for our picture to occur. For example, taking the parameters of Cyg X-3, $x_o \geq 3r_s$ and $T_s \geq 9\times10^4$K (Moffat & Marchenko 1996). They give $A \approx 10^{44.4}$ erg s^{-1} K^{-2} (Fig. 3) and the luminosity for which the cascade can be initiated by VHE γ-rays: $L_s^{\tau=1} \approx 2\times10^{34}$erg s^{-1}. This is much less than the typical luminosity of Wolf-Rayet stars. Similarly, for LSI 303^o+61 binary system, taking $x_o \approx 5r_s$ and $T_s \approx 2.6\times10^4$K (Hutchings & Crampton 1981), $A \approx 10^{44.4}$erg s^{-1} K^{-2} and $L_s^{\tau=1} \approx 4\times10^{35}$erg s^{-1}, which is much less than the luminosity of a massive star in LSI 303^o+61, equal to $\sim 10^{38}$erg s^{-1}. Detailed analysis of the γ-ray light curves expected from these two and other massive binaries (e.g. Cyg X-1), using available information on the parameters of these systems, will be reported in the next paper (Bednarek et al. 1996).

Acknowledgements. This work is supported by the University of Lódź grant no. 505/491.

Appendix A: the propagation distance and the optical depth for γ-ray photons in the radiation field of a massive companion

Let us assume that γ-ray photon with energy E_γ is injected at a distance x_o from the center of a massive star at an angle α. The characteristic propagation distance for this γ-ray photon can be defined as

$$\lambda_{\gamma\gamma}^{-1}(E_\gamma, x_o, \alpha) = \int d\mu(1+\mu)\int d\phi \int_0^\infty \frac{n(\epsilon,\Omega)}{d\epsilon d\Omega dV} \sigma_{\gamma\gamma}(\beta)d\epsilon, \quad \text{(A1)}$$

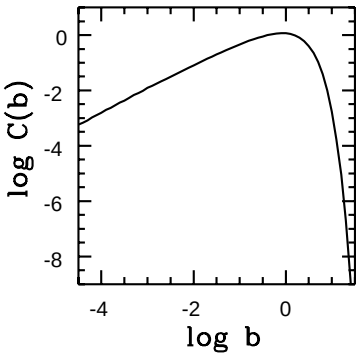

Fig. 10. The dependence of $C(b)$ on b.

where μ is the cosine of the angle between colliding photons, $n(\epsilon,\Omega,l)/d\epsilon d\Omega dV$ is the differential density of photons with energy ϵ coming from a massive star, $\sigma_{\gamma\gamma}(\beta)$ is the cross section for $e^{\pm}$ pair production in two photon collision (Jauch & Rohrlich 1955), and $\beta^2 = 1 - a/\epsilon$, with $a = 2m_e^2/E_\gamma(1+\mu)$.

The above formula can be written in a simpler form

$$\lambda_{\gamma\gamma}^{-1}(E_\gamma, x_o, \alpha) = 4S(kT)^3\sigma_T \int_{\mu_{min}}^{\mu_{max}} (1+\mu) \phi(\mu) C(b) d\mu, \quad \text{(A2)}$$

where $2\phi(\mu)$ is the result of analytical integration over ϕ and is given by the spherical trigonometry relations, $b = a/(kT)$ is a dimensionless parameter, T, k, σ_T are the star surface temperature, the Boltzmann constant, and the Thomson cross section, and $S = 2(hc)^{-3}$. $C(b)$ depends only on the parameter b and is given by

$$C(b) = \frac{3}{16} b^3 \int_0^1 \frac{\beta}{(1-\beta^2)^3} \frac{1}{e^{b/(1-\beta^2)} - 1} [(3-\beta^4)\ln(\frac{1+\beta}{1-\beta}) - 2\beta(2-\beta^2)] d\beta. \quad \text{(A3)}$$

$C(b)$ has been computed numerically and its dependence on b is shown in Fig. 10.

The optical depth for the γ-ray photon in the radiation field of a star is obtained from

$$\tau(E_\gamma, x_o, \alpha) = \int_0^\infty \lambda_{\gamma\gamma}^{-1}(E_\gamma, x_o, \alpha) dl \quad \text{(A4)}$$

where l is the distance measured along the photon path from x_o and at an angle α.

Appendix B: the spectra of $e^{\pm}$ pairs produced by γ-rays in collisions with the radiation field of a massive companion

The spectra of $e^{\pm}$ pairs created per unit path length by γ-ray photon, with energy E_γ, interacting with the star photons at the distance x_o and the propagation angle α, can be obtained from

$$\frac{dW(E_\gamma, x_o, \alpha)}{dEdx} = \int d\mu(1+\mu) \int d\phi \int \frac{n(\epsilon,\Omega,l)}{d\epsilon d\Omega dV} \sigma(E_\gamma, E, \mu) d\epsilon, \quad \text{(B1)}$$

where the differential density of star photons and the integrations over $d\mu$ and $d\phi$ are defined as in Appendix A, and $\sigma(E_\gamma, E, \mu)$ is the differential cross section for production of electron (positron) with energy E in two photon collision (Akhiezer & Berestetskii 1965).

Since the integral over $d\epsilon$ can be parametrized after some modifications, we can rewrite the above formula into the form:

$$\frac{dW(E_\gamma, x_o, \alpha)}{dEdx} = \frac{3m_e^2 S\sigma_T (kT)^2}{4\pi E_\gamma^2} \int_{\mu_{min}}^{\mu_{max}} (1+\mu) \phi(\mu) D(\chi,\eta) d\mu, \quad \text{(B2)}$$

where the dimensionless parameters η and χ are defined by

$$\eta = E/E_\gamma, \quad \text{(B3)}$$

and

$$\chi = 2(kT)E_\gamma(1+\mu)m_e^{-2}. \quad \text{(B4)}$$

The function $D(\chi,\eta)$ is given by

$$D(\chi,\eta) = \int_{(\chi\eta(1-\eta))^{-1}}^\infty \frac{zF(z)}{e^z - 1} dz, \quad \text{(B5)}$$

with

$$F(z) = \frac{2\rho - 1 + (\rho-1)A^2(\chi,\eta)}{B^2(\chi,\eta) + \rho A^2(\chi,\eta)} - \frac{2(\rho-1)^2 A^4(\chi,\eta)}{[B^2(\chi,\eta) + \rho A^2(\chi,\eta)]^2}, \quad \text{(B6)}$$

where

$$B^2(\chi,\eta) = (1-2\chi)^2\rho(\rho-1)^{-1}, \quad \text{(B7)}$$

$$A^2(\chi,\eta) = 1 - B^2(\chi,\eta), \quad \text{(B8)}$$

and $\rho = 0.25\chi z$. $D(\chi,\eta)$ has been computed numerically and its dependence on η is shown in Fig. 11 for selected values of χ.

Appendix C: the spectra of γ-ray photons produced by $e^{\pm}$ pairs in ICS of low energy photons from a massive companion

The approximate spectra of γ-rays produced by electrons with the energy E (and the Lorentz factor γ) are obtained following the general prescription given by Jones (1968) (see also

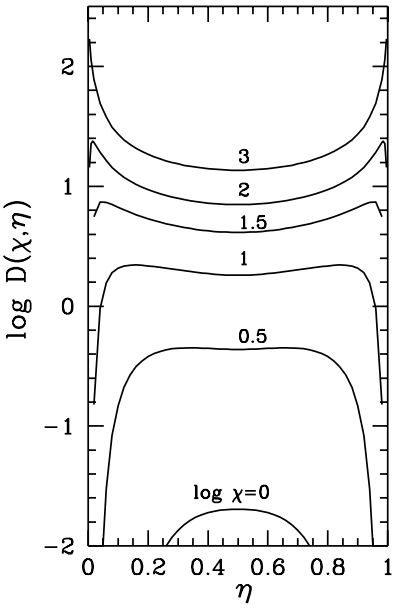

Fig. 11. The dependence of $D(\chi, \eta)$ on η for selected values of χ.

Blumenthal & Gould 1970). However we have to modify this method in order to obtain the γ-ray spectra in the case of anisotropic background radiation field which is defined by the parameters of a massive companion, the distance x_0 between electron (positron) and the star, and the angle of propagation α. Using Eq. 2-6 in Jones (1968), we can write the formula for γ-ray spectra into the form:

$$\frac{dN}{dtdE_\gamma} = \frac{r_0^2 c E_\gamma}{2\gamma^4 (m_e c^2)^3 (1 - E_\gamma/E)} \int \frac{d\epsilon}{e^{\epsilon/kT} - 1} \int \phi(\mu) d\eta \; [\eta^2 - 2\eta + 2 + \frac{(E_\gamma/E)^2}{(1 - E_\gamma/E)}] \frac{S(\eta; \eta_1, \eta_2)}{\eta^2}, \qquad \text{(C1)}$$

where $\mu \cong E_\gamma m_e c^2/(\epsilon\gamma(E - E_\gamma)\eta) - 1$ for $\gamma >> 1$, ϵ is the energy of a photon coming from the star, $\phi(\mu)$ is determined as in Appendix A, $S(\eta; \eta_1, \eta_2)$ is defined in Jones (1968). $\eta_{1,2} = E_\gamma/[\epsilon\gamma(1+\beta\cos\theta_{1,2})(E-E_\gamma)]$, where $\theta_{1,2}$ are the angles between the electron (positron) direction and two limbs of the star. The integration over η should be performed over the part of interval η_1 to η_2 which lays at least partially within $\eta_L = 1 - \beta$ and $\eta_U = 1 + \beta$.

References

Akhiezer, A.I., Berestetskii, V.B. 1965, Quantum Electrodynamics, New York: Interscience

Barker, P.K. 1986, PASP 98, 44

Bednarek, W., Giovannelli, F., Karakula, S., Tkaczyk, W. 1990, A&A 236, 175

Bednarek, W. et al. 1996, in preparation

Bignami, G.F., Maraschi, L., Treves, A. 1977, A&A 55, 155

Blumenthal, G.R., Gould, R.J. 1970, Rev.Mod.Phys. 42, 237

Eichler, D., Usov, V. 1993, ApJ 402, 271

Fichtel, C.E., Thompson, D.J., Lamb, R.C. 1987, ApJ 319, 362

Gould, R.J., Schreder, G.P. 1967, Phys. Rev. 155, 1408

Harding, A.K., Gaisser, T.K. 1990, ApJ 358, 561

Hermsen, W. et al. 1977, Nat 269, 494

Hermsen, W. et al. 1987, A&A 175, 141

Hutchings, J.B., Crampton, D. 1981, PASP 93, 486

Jauch, J.M., Rohrlich, F. 1955, The theory of photon and electrons, Addison-Wesley

Jones, F.C. 1968, Phys.Rev. 167, 1159

Lamb, R.C. et al. 1977, ApJ 212, L63

Ling, J.C., Wheaton, W.A. 1989, ApJ 343, L57

Maheswaran, M., Cassinelli, L.P. 1988, ApJ 335, 931

Merck, M., Kanbach, G., Mayer-Hasselwander, H.A., Meintjes, P. 1995, Proc. 24th ICRC (Rome), v. 2, p.190

Moffat, A.E.J., Marchenko, S.V. 1996, A&A 305, L29

Moskalenko, I.V., Karakula, S., Tkaczyk, W. 1993, MNRAS 260, 681

Thompson, D.J., Bertsch, D.L., Dingus, B.L. et al. 1995, ApJS 101, 259

Usov, V.V. Melrose, D.B. 1992, ApJ 395, 575

van Dijk, R., Bloemen, H., Hermsen, W. et al. 1993, COMPTEL PREPRINT No. 11, p. 7

van Kerkwijk, M.H. et al. 1992, Nat 355, 703

Vestrand, W.T., Eichler, D. 1982, ApJ 261, 251

Weber, E.J., Davis, L., Jr. 1967, ApJ 148, 217

Weekes, T.C. 1988, Phys. Rep. 160, 1

Weekes, T.C. 1992, Space Sci. Rev. 59, 314

This article was processed by the author using Springer-Verlag LaTeX A&A style file *L-AA* version 3.